Revisiting tolerance to ocean acidification: Insights from a new framework combining physiological and molecular tipping points of Pacific oyster

Mathieu Lutier, Carole Di Poi, Frédéric Gazeau, Alexis Appolis, Jérémy Le Luyer, Fabrice Pernet

Revisiting tolerance to ocean acidification: insights from a new framework combining physiological and molecular tipping points of Pacific oyster

Mathieu Lutier[1,*], Carole Di Poi[1], Frédéric Gazeau[2], Alexis Appolis[1], Jérémy Le Luyer[3], Fabrice Pernet[1,*]

[1] LEMAR CNRS/UBO/IRD/Ifremer, ZI pointe du diable, CS 10070, F-29280 Plouzané, France.

[2]LOV Sorbonne Université, CNRS, Laboratoire d'Océanographie de Villefranche, Villefranche-sur-Mer, France.

[3]EIO UPF/IRD/ILM/Ifremer, Labex CORAIL, Unité RMPF, Centre Océanologique du Pacifique, Vairao – BP 49 Vairao, Tahiti, Polynésie française.

Correspondence and requests for materials should be addressed to Fabrice Pernet (email: fpernet@ifremer.fr)

For submission to global change biology.

Abstract

Studies on the impact of ocean acidification on marine organisms involve exposing organisms to future acidification scenarios which has limited relevance for coastal calcifiers living in a mosaic of habitats. Identification of tipping points beyond which detrimental effects are observed is a widely generalizable proxy of acidification susceptibility at the populational level. This approach is limited to a handful of studies that focus on only a few macro-physiological traits, thus overlooking the whole organism response. Here we develop a framework to analyze the broad macro-physiological and molecular responses over a wide pH range in juvenile oyster. We identify low tipping points for physiological traits at pH 7.3-6.9 that coincide with a major reshuffling in membrane lipids and transcriptome. In contrast, a drop in pH affects shell parameters above tipping points, likely impacting animal fitness. These findings were made possible by the development of an innovative methodology to synthesize and identify the main patterns of variations in large -omic datasets, fitting them to pH and identifying molecular tipping-points. We propose the broad application of our framework to the assessment of effects of global change on other organisms.

Keywords

Acidification, Lipidomic, Mollusk, Reaction norm, Threshold, Transcriptomic

41 **Introduction**

42 The exponential increase in the atmospheric emission of carbon dioxide (CO_2)
43 from anthropogenic activities is mitigated by ocean absorption that leads to decreasing
44 ocean pH and changes in carbonate chemistry, a phenomenon known as ocean
45 acidification (OA) (Caldeira & Wickett, 2003; Orr et al., 2005). This represents a
46 tremendous challenge for marine organisms, especially for calcifiers that produce calcium
47 carbonate ($CaCO_3$)-based exoskeletons. OA not only induces internal acidosis that
48 impacts metabolism, behavior, growth and reproduction, but also decreases carbonate ion
49 (CO_3^{2-}) concentration in the ocean, the elemental constituent of calcifier exoskeletons
50 (Gazeau et al., 2013; IPCC, 2019; Kroeker et al., 2013; Tresguerres & Hamilton, 2017
51 for reviews).

52 OA has been the most-studied topic in marine science in recent times (Browman,
53 2017). As such, many OA experiments have been conducted, usually exposing organisms
54 to experimental conditions based on scenarios modelled for open ocean waters, typically
55 simulating present and near-future surface ocean pH levels. However, many calcifying
56 species thrive in coastal areas where pH levels vary far more than in the open ocean on
57 both daily and seasonal scales (Vargas et al., 2017; Waldbusser & Salisbury, 2014). As a
58 result, several authors have applied pH offsets or conditions that are more locally relevant
59 (Dineshram et al., 2015; Gazeau et al., 2014; Ko et al., 2014), but the results cannot be
60 extrapolated to populations or species that are distributed in a mosaic of habitats. We need
61 to implement experimental approaches whose results can be applied in a wide range of
62 environments at the scale of species (Vargas et al., 2017).

63 Reaction norm, i.e. the response of an organism to changing environmental
64 parameters, allows the identification of tipping points that beyond small variations will
65 have major impacts. According to the last IPCC reports, identification of tipping-points

66 is a key knowledge gap in environmental change research (IPCC, 2019, 2021). Tipping-
67 point is valid for a whole population regardless of habitat. Also, this is a single, easily
68 communicable value that reflects susceptibility to OA (Bednaršek et al., 2019, 2021). To
69 date, only four studies have experimentally established reaction norms for marine
70 calcifiers in relation to pH. These studies focused on the assessment of tipping points for
71 a few selected traits measured at the organism level (i.e. growth, survival) and provide a
72 limited view of the whole organism response, ignoring molecular responses (Comeau et
73 al., 2013; Dorey et al., 2013; Lee et al., 2019; Ventura et al., 2016). We therefore identify
74 the need to integrate macro-physiology and omics together with reaction norms, for
75 understanding the mechanisms responsible for individual organism success under a
76 changing environment. This however requires developing an innovative methodology to
77 synthesize and identify the main patterns of variations in large -omics datasets (Strader et
78 al., 2020) and fit them to reaction norms.
79 Lipidomic and transcriptomic approaches provide complementary and holistic
80 views of organismal responses to environmental changes at the molecular and
81 biochemical levels. Membrane lipids modulate exchanges between the intracellular
82 milieu, which is highly-regulated, and the extracellular milieu which reflects
83 environmental changes, and therefore play a key role in metabolic regulation and ion
84 exchanges (Hazel & Williams, 1990; Hochachka & Somero, 2002; Hulbert & Else, 1999).
85 However, the role of membrane lipids in the regulation of acid-base equilibrium and
86 biomineralization under OA has never been investigated. Here we expect that membrane
87 lipids play a key role in the maintenance of electrochemical gradient across membranes,
88 a parameter that is essential for organism's persistence under OA (Cyronak et al., 2016).
89 The transcriptomic response is one of the first level of metabolic regulation that
90 determine shifts in acid-base ion regulation, metabolic processes, calcification and stress

response mechanisms (Matz, 2018; Strader et al., 2020). Although an increasing number of studies investigate the transcriptomic responses of marine calcifiers under OA, they generally focus on a few targeted genes that play a central role in physiological processes and they assume that gene functions are conserved among taxa (Strader et al., 2020). This creates a vicious cycle limiting the opportunities to uncover new mechanisms and cellular pathways involved in organism responses to OA. New methodologies are therefore required to provide new insight on organism's response to OA at the transcriptional level (Rajan et al., 2021; Yarra et al., 2021).

Here we determine the reaction norm of juvenile Pacific oyster *Crassostrea gigas*, one of the most cultivated invertebrate species in the world (FAO, 2020), over a wide range of pHs for macro-physiological traits, membrane lipids and gene expression. Although the impacts of OA on this model species have been intensively studied using scenario approaches, there is currently no consensus on its robustness to low pH (Ducker & Falkenberg, 2020). The establishment of reaction norm with biochemical and molecular data is a novel approach that provides new insights on the sensitivity of marine calcifiers to OA.

Material and methods

Animals and maintenance

The oysters were produced at the Ifremer hatchery facilities in Argenton (Brittany, France) in late August 2018 according to Petton et al. (2015). The broodstock consisted of 139 females and 40 males originating from six different cohorts collected in the natural environment between 2011 and 2016, off Fouras (Ile d'Aix, France). At 40 days old, the juveniles were moved to the Ifremer growing facilities in Bouin (Vendée, France). On January 10th 2019, oysters were returned to Argenton and kept for 8 d in a 500 L flow-

115 through tank. Seawater temperature was gradually increased from 7 °C to 22 °C, the
116 optimal temperature for *C. gigas* (Bayne, 2017), at a rate of *ca.* 2 °C d^{-1}. During the
117 experiment, oysters were continuously supplied with natural seawater originating from
118 a pool (~9000 m^3) which is renewed with each spring tide, filtered at 5 µm and UV-
119 treated. The oysters were fed continuously on a mixed diet of *Isochrysis affinis galbana*
120 (CCAP 927/14) and *Chaetoceros gracilis* (UTEX LB2658) (1:1 in dry weight). Food
121 concentration was maintained at 1500 μm^3 mL^{-1} of phytoplankton cells at the outlet
122 of the tank – *ad libitum* (Rico-Villa et al., 2009) – and controlled twice daily using an
123 electronic particle counter (Multisizer 3, Beckman Coulter, USA) equipped with a 100
124 µm aperture tube. On the eve of the experiment on January 14th 2019, at which point
125 they were 5-month-old, oysters were divided into 15 batches containing 292 ± 20
126 individuals (95.2 ± 0.2 g).

127 **Experimental design**

128 Each batch of oysters was exposed to one constant nominal pH condition ranging from
129 pH 7.8 to 6.4 with a step of 0.1 between two levels. The upper pH condition (pH ~7.8)
130 was obtained by running seawater with oysters without pH regulation. The lowest pH
131 values encountered by oysters today are presumably between pH 7.4 and 7.0
132 (Frankignoulle et al., 1996; Melzner et al., 2013; Proum et al., 2017; Wallace et al., 2014).
133 Geochemical models using the record of atmospheric CO_2 levels over the last 300 Myr
134 suggest that the ocean pH was at most 0.6 units lower than today (Caldeira 2003).
135 Continued release of CO_2 from fossil fuels into the atmosphere (worst case scenario)
136 could result in a reduction in pH of 0.7 units at the ocean surface (Caldeira 2003).

Therefore, the lowest pH values used in our study are probably unrealistic but expand the reaction norms and increase the statistical power of the tipping point.

The experimental system consisted of 18 experimental units that were randomly assigned to one pH condition (n = 15, no pH replication) or to control blanks without animals (n = 3) (Supplementary Figure 1). Each experimental unit consisted of a header tank in which seawater was acidified (except for the ambient pH and blanks) and then delivered by a pump to a holding tank containing the oysters. These tanks were 45 L and their entire volume was renewed every 82 min. pH was regulated by means of pure-CO_2 bubbling, controlled by a pH-regulator (ProFlora® u403 JBL). The pH-regulator was connected to pH-probes installed in each header tank (pH-sensor+Cal, JBL), checked at the start of the experiment using Certipur® Merck NBS buffers (pH = 4.00, pH = 7.00). pH electrodes from the pH-regulator were inter-calibrated twice daily against a pH probe (Sentix® 940-3 WT) connected to a Multiline® Multi 3630 IDS-WTW. The pH-probe was checked once a week using Certipur® Merck NBS buffers (pH = 4.00, 7.00, and 9.00) and calibrated twice a week on the total scale with a certified Tris/HCl buffer (salinity 35; provided by A. Dickson, Scripps University, USA). Throughout the text, pH levels are therefore expressed on the total scale (pH_T). In each experimental tank, air bubbling and a small homogenisation pump (3 W) ensured an efficient mixing of seawater surrounding the oysters. Photoperiod was 10 h light: 14 h dark. During the entire experimental period, oysters were fed as described above.

158 On January 18th 2019, each batch of oysters was randomly assigned to one tank.
159 Oysters were first held at ambient pH for 3 d. Then, pH was progressively decreased in
160 each pH-regulated tank at a rate of 0.2 unit d^{-1}. The decrease in pH lasted for 7 d for the
161 lowest condition. Experimental pH conditions were all reached on January 27th 2019.
162 The pH exposure lasted 23 days, the time required for critical shell alteration
163 (bleaching, perforation, and dissolution) under the lowest pH conditions. No mortality
164 was recorded during the experiment.

165 **Seawater carbonate chemistry**

166 In each oyster tank, temperature, salinity, dissolved oxygen (O_2) saturation
167 levels and pH were measured twice a day using a Multiline® Multi 3630 IDS-WTW
168 (pH probe Sentix® 940-3 WTW, O_2 probe FDO® 925 WTW, salinity probe TetraCon®
169 925 WTW). Seawater samples were collected weekly, filtered through 0.7 µm (GF/F,
170 Whatman®) and poisoned with 0.05% mercury (II) chloride. Total alkalinity (TA) was
171 then measured in triplicate 50 mL subsamples by potentiometric titration at 22 °C,
172 using a Titrando 888 (Metrohm®) titrator coupled to a glass electrode (ecotrode plus,
173 Metrohm®) and a thermometer (pt1000, Metrohm®). TA was calculated following the
174 protocol described in Dickson et al. (2007). At the time of sampling, pH, salinity and
175 temperature were measured, and then used together with TA value to determine
176 carbonate chemistry parameters using the package seacarb v 3.2.16. of the R software.

177 **Biometry**

178 The total fresh weight (shell + tissue) of each batch of oysters was measured
179 twice weekly and interpolated between measurements to estimate daily weight. In

addition, shell length and total fresh weight were measured individually on 30 oysters from each condition at the onset (1 d) and at the end of the experiment (23 d). The measurements relate to different individuals taken over time. These oysters were then dissected and pooled to determine the total weight of shell and tissue, separately. The tissues were then lyophilized and weighted to obtain dry weight. Growth rate was calculated as:

$$G = \left(\overline{X_{23}} - \overline{X_1}\right) \div 23,$$

where G is growth rate as expressed as increase in shell length or total body weight per day (mm d^{-1}, mg TW d^{-1}), $\overline{X_1}$ and $\overline{X_{23}}$ are the average parameter values for shell length and total weight measured at the onset (1 d) and the end of the experiment (23 d).

Shell thickness was measured on the left valve of five individuals collected per pH condition at the end of the experiment. The left valve was more susceptible to acidification than the right valve. We observed holes in the shell under low pH condition (pH < 6.6) that always occurred on the left valves, close to the umbo. Shells were dried for 24 h at 45 °C, embedded in polyester resin and cross-sectioned from umbo to opposite shell margin along the longitudinal growth axis using a precision saw (Secotom-10 Struers). Sections were glued on a microscope slide and polished with silicon carbide abrasive disks (1200 and 2500 grains cm^{-2}). Images of the section were captured under a Lumar V12 stereoscope (Zeiss) at 30x magnification, and the entire section was reconstructed using an image acquisition software (AxioVision SE 64 –

v4.9.1, Zeiss). The minimal shell thickness was measured within the first third of the shell starting from umbo using ImageJ software (Schneider et al., 2012).

Physiological rates

Seawater was sampled twice a day at the inlet and outlet of each oyster tank and phytoplankton cell concentrations were measured using an electronic particle counter (see previous section). No pseudofaeces production was detected throughout the experiment. Ingestion rate was determined as:

$$I = \frac{\Delta_{phyto} \times \text{flow rate}}{W},$$

where I is the ingestion rate expressed as $cm^3\ min^{-1}\ g^{-1}$, Δ_{phyto} is difference in phytoplankton concentrations between the inlet and the outlet of the oyster tanks ($cm^3\ min^{-1}$), *flow rate* is the water flow at the inlet of the oyster tanks ($mL\ min^{-1}$), and W is the total fresh weight of oyster batch (g). The three control blanks were used to check that there was no sedimentation of algae (no differences in cell concentrations between the inlet and the outlet, data not shown).

Net calcification and respiration rates were measured after 22 d of exposure. Food supply was stopped 17 h before the assay and tanks were emptied, cleaned and refilled. Again, 1 h before the assay, the tanks were emptied, cleaned and refilled. At the onset of the incubation, water flow and air bubbling were stopped. Gentle mixing of the seawater was maintained by homogenization pump but air bubbling was stopped. Incubations lasted for 90 min. This duration allowed to keep the pH close to the setpoint (< 0.1 pH unit variation) despite oyster respiration. At the onset and at the end of the incubation period, temperature, salinity, pH and O_2 concentration (mg

223 L^{-1}) were measured, and seawater samples were filtered and poisoned for TA analyses
224 (see above) or were immediately frozen at -20 °C for ammonium (NH_4^+) measurements
225 (Aminot & Kérouel, 2007) (see Supplementary Table 1). Empty tanks were used as
226 controls to check that there was no change in any of the parameters due to
227 evaporation or other potential biological processes in the water itself. Net calcification
228 rate was determined following a modified procedure from Gazeau et al. (2015) using
229 the alkalinity anomaly technique (Smith & Key, 1975):

230 $$NC = \frac{(\Delta_{TA} \times \rho - \Delta_{NH_4^+}) \times V}{2 \times t \times W \times \frac{DW}{TW}},$$

231 where NC is the net calcification rate expressed as μmol $CaCO_3$ h^{-1} g^{-1}, Δ_{TA} and Δ_{NH4+}
232 are differences in TA (μmol Kg^{-1}) and NH_4^+ (μmol L^{-1}) between the onset and the end
233 of the incubation period, ρ is seawater density (kg L^{-1}) calculated based on temperature
234 and salinity during the incubation, V is the volume of the tanks (L), t is the duration
235 of the incubations (h), $\frac{DW}{TW}$ is the ratio of dry weight and total weight determined after
236 lyophilization of a pool of tissues from 30 oysters (see above).
237 Respiration rate was determined following:

238 $$R = \frac{(\Delta_{O_2} - \Delta_{O_2\ Control} \times \rho) \times V}{t \times W \times \frac{DW}{TW}},$$

239 where R is the respiration rate expressed as mg O_2 h^{-1} g^{-1}, Δ_{O_2} and $\Delta_{O_2\ Control}$ are
240 differences in O_2 concentration (mg L^{-1}) between the onset and the end of the
241 incubation period in the oyster tank and in the three control tanks (average)
242 respectively. Negative values mean that oxygen consumption was negligible and
243 similar to control blanks.

Biochemistry

Soft-tissues of five individuals from each pH condition were collected at 23 d, flash-frozen in liquid nitrogen, pooled, grounded with a ball mill and stored at -80 °C pending analyses. Oyster powder was diluted with chloroform/methanol (2:1, v/v) for the determination of neutral lipids (triacylglycerol: TAG, and sterols: ST) using high performance thin layer chromatography. TAG-ST ratio was used as a proxy of the relative contribution of lipid reserve to structure (membrane). Polar lipids were purified on silica gel micro column, transesterified using methanolic H_2SO_4 at 100 °C, and the resulting fatty acid methyl esters (FAME) were analyzed using a gas-chromatography flame ionization detection system equipped with a DB-Wax capillary column. Peaks were analyzed by comparison with external standards. Each fatty acid was expressed as the peak area percentage of total polar fatty acids. Carbohydrate content (μg mg^{-1}) was determined according to the colorimetric method described in DuBois et al. (1956).

Transcriptomics

Soft-tissues of five individuals from each tank were collected at 23 d, flash-frozen in liquid nitrogen and individually grounded (n = 75). Total RNA was then extracted with Extract-All (Eurobio) at a ratio of 5 mL per 100 mg of tissue. RNA quantity/integrity and purity were verified with a NanoDrop 2000 spectrophotometer (Thermoscientific®) and a Bioanalyzer 2100 (Agilent Technologies®) respectively. Samples were then DNase-treated using a DNase Max™ Kit (MO BIO Laboratories, Inc.) and analyzed at the Genotoul sequencing platform (INRAE US 1426 GeT-PlaGe,

Centre INRAE de Toulouse Occitanie, Castanet-Tolosan, France). TruSeq RNA libraries were multiplexed and sequenced on a single lane of NovaSeq6000 Illumina S4 150-bp paired-end.

Raw reads were first filtered using Trimmomatic v.0.36 for a minimum length (60 bp), a minimum quality (trailing = 20, leading = 20) and the presence of potential contaminants and remaining adaptors (https://ftp.ncbi.nlm.nih.gov/pub /UniVec; 08/17/20). The quality of the reads was monitored before and after this trimming process with FastQC v.0.11.5 (https://www.bioinformatics.babraham.ac.uk/projects/fastqc/). The *C. gigas* reference genome (Peñaloza et al., 2021) was downloaded from NCBI (GCF_902806645.1) and indexed with Gmap v2020.06.01. Filtered reads were mapped against the reference genome using GSNAP v2020-06-30 keeping default parameters but allowing a minimum mismatch value of 2 and a minimum read coverage of 90%. Finally, the gene expression levels were assessed using HTSEQ v0. 6.1. The DESeq2 v1.30.0 R package was used to process the expression with a first step of normalization using the variance-stabilizing transformation implemented in the *'vst'* function. The *vst* matrix was used to build a signed weighted co-expression network analysis implemented in the WGCNA v1.69 R package. First, genes with low overall variance (< 5%) were removed for the analysis as recommended (Langfelder & Horvath, 2008). We fixed the "soft" threshold powers of 13 the scale-free topology criterion to reach a model fit (|R|) of 0.90. Clusters were defined using the "*cutreeDynamic*" function (minimum of 50 genes by cluster and default cutting height of 0.99) based on the topological overlap

matrix, and an automatic merging step with the threshold fixed at 0.25 (default) allowed merging correlated clusters. For each cluster, we defined the cluster membership (kME; Eigengene-based connectivity) and only clusters showing significant correlation ($p < 0.01$) to pH were kept for downstream functional analysis.

Statistical analysis

All statistical analyses were performed using the R software v4.0.3 and the threshold of statistical significance was fixed at 0.05 unless specifically stated. Relationships between dependent variables and average pH recorded during the exposure period (or the incubation period for net calcification and respiration rates) were computed using regression models. Dependent variables were biometrics (shell length, total body weight, and growth), physiological rates (ingestion, net calcification and respiration), biochemistry (lipid reserves, carbohydrates) and gene expression. Each gene included in the WGCNA clusters were individually tested against pH. Fatty acids were summarized using principal component analysis and separated into two groups according to their correlation with first principal component (positive or negative). Each group was then summed and tested against pH. Piecewise, linear and log-linear regression models were tested and compared for each individual variable (or set of variables). In each case, the model that had the highest R^2, the lowest Akaike and Bayesian information criteria (AIC, BIC) and the lowest residual sum of squares was selected. For each piecewise regression model, we estimated the tipping point, defined as the values of the pH where the dependent variables tip, by implementing the bootstrap restarting algorithm (Wood, 2001). For physiological rates, we also

406 determined the critical-point defined as the pH at which the dependent variable was
407 equal to zero. Normality of residual distribution was tested using Shapiro-Wilk test
408 and homogeneity of variances was graphically checked. Significance of each slope was
409 tested according to Student's *t* test. Piecewise regression models were built using the
410 segmented v1.3-4 R package.
411 For transcriptomic analysis, only genes that are significantly correlated to pH were tested
412 among the retained clusters (Pearson correlation). The frequency distribution of pH
413 tipping-point values was plotted for each cluster of genes. Groups of genes which exhibit
414 neighboring tipping points with distribution frequencies > 5%, were grouped together and
415 used for GO enrichment analysis using GOA-tools v0.7.11 (Klopfenstein et al., 2018),
416 implemented in the Github repository '*go_enrichment'*
417 (https://github.com/enormandeau/ go_enrichment) and the go-basic.obo database
418 (release 2019-03-19) with Fisher's extract tests. Only significant GO terms that
419 included a minimum of three genes and with Bonferroni adjusted $P < 0.01$ were kept.
420 For complementarity with previous studies, we also specifically examined the genes
421 that are commonly reported as involved in the calcification process and in the
422 formation of the organic matrix of the shell and periostracum (Supplementary File 1).

423 **Results**

424 **Acclimation of oysters to 15 different pH conditions**

425 During the experiment, pH levels in the oyster tanks were stable and reached the
426 targeted values, except for the lowest pH condition that was 6.5 ± 0.3 instead of 6.4
427 (Supplementary Note 1, Supplementary Table 2, Supplementary Figure 2). The effects of
428 acidification were clearly visible at the end of the experiment on the color and the

size of the shells, as shown in Figure 1. Shell pigmentation apparently decreased with decreasing pH. Total body weight and shell length of oysters ranged from 0.4 ± 0.1 to 2.0 ± 0.8 g and from 12.9 ± 2.1 to 25.4 ± 4.5 mm respectively (mean ± SD; Figure 2A, Supplementary Figure 3).

Most macro-physiological traits tip at low pH values between 7.1-6.9

We measured biometric parameters like the length, thickness, and weight of the shell and the total body weight and the dry flesh weight at the end of the 23-day exposure to the 15 different pH conditions. We calculated growth rates for shell length and total body weight, and we measured physiological rates like calcification, ingestion and respiration rates. From these data, we identified an overall tipping point for macro-physiological traits at pH ~7.1-6.9 below which they declined sharply (Figures 2A-H). Calcification rate and growth rates exhibited critical points at pH 6.8 and 6.6, respectively, below which they became negative and turned to net dissolution of the shell and weight and length losses (Figures 2B-D). Concomitantly, respiration rate was arrested at pH 6.7 and ingestion rate was near-zero at pH 6.5 (Figure 2E-F).

Shell parameters and respiration rate are impacted above tipping point

Although macro-physiological traits were generally unaffected by reductions in pH above tipping points, this was not the case for shell length, shell weight and respiration rate. Both shell parameters indeed decreased with decreasing pH while the respiration rate increased before reaching the tipping point (Figures 2A, 2E and 2G). In addition, the shell thickness was the only parameter that decreased linearly over the entire pH range without demonstrating a measurable tipping point (Figure 2I).

A major remodeling of membrane lipids occurs at pH 6.9

To provide an in-depth characterization of the reaction norms at the whole organism level, we aimed to link the oyster reaction norm established for the macro-physiological traits described previously to the molecular responses of oysters. We first analyzed the fatty acid composition of membrane lipids that play an important role in exchanges between intracellular and extracellular compartments. Principal component analysis of all fatty acids showed that the first axis (PC1) alone explained 66% of the total variance in relation to pH (Figure 3A). The set of fatty acids was reduced to two terms defined by the sums of fatty acids that correlated with PC1 either positively or negatively, and each term was plotted against pH (Figure 3B-C). Positively correlated fatty acids mainly consisted of docosahexaenoic acid (DHA, 22:6n-3) and palmitic acid (PA, 16:0) contributing 43% and 14%, respectively, to PC1 (Supplementary Table 3). This group of fatty acids exhibited a tipping point at pH 6.9, below which their contribution to membranes decreased markedly (Figure 3B). In contrasts, the contribution to membrane of the fatty acids that were negatively correlated with PC1 increased markedly below pH 6.9. These negatively correlated fatty acids consisted of arachidonic acid (ARA, 20:4n-6), eicosapentaenoic acid (EPA, 20:5n-3) and non-methylene interrupted fatty acids (22:2NMI$_{i,j}$), which contributed 12%, 6% and 6%, respectively, to PC1 (Figure 3C) (Supplementary Table 3).

Expression of most genes shows tipping points at pH 7.3-6.9

To further assess the molecular effects of pH change, we compared the transcriptome responses of oysters exposed to the 15 pH conditions for 23 days using RNA-seq. To do this, we first clustered the differentially expressed genes that co-vary together using WGCNA analysis and retained the clusters that were correlated with pH (Supplementary Table 4). Then, we plotted the frequency distribution of pH tipping-point

for each cluster of genes (Figure 4). Owing to this original method, we found that 1054 genes, distributed in three clusters, showed linear (or loglinear) or piecewise regression with pH (Supplementary Table 4). Among them, 49% showed tipping-points at pH 7.3-6.9 (Figure 4A-C). Expression level of most genes were unchanged between pH conditions down to the pH tipping point, below which it increased for genes in clusters 1 and 2 (Figure 4A-B), or decreased for genes in cluster 3 (Figure 4C). Some genes linearly increased for clusters 1 and 2, or decreased for cluster 3 with decreasing pH.

Gene ontology analysis (GO) showed that most of the genes from cluster 1 (42%) exhibited tipping-points at pH 7.3-6.9 (Figure 4A) and were associated with GO terms corresponding to the regulation of RNA-transcription, cellular metabolism, macromolecule biosynthesis and negative regulation of cell-cell adhesion (Table 1). The expression of another group of genes from cluster 1 (14%) increased linearly (or loglinearly) with decreasing pH and was associated with GO terms corresponding to GTP-binding, GTPase activity and ribonucleotide metabolism (Table 1). The expression of most of the genes from cluster 2 (44%) exhibited tipping-points at pH 7.3- 7.0, whereas another large group of genes (18%) increased linearly (or loglinearly) with decreasing pH (Figure 4B). These genes were associated with GO terms corresponding to ribosome synthesis, RNA-binding, translation and protein/amino acid synthesis (Table 1). The expression of 62% of the genes from cluster 3 exhibited tipping-points at pH 7.2-6.9 and decreased thereafter (Figure 4C). These genes were associated with GO terms corresponding to ion transport and more specifically to transmembrane cation transport (Table 1).

Expression of genes related to biomineralization shows tipping point at pH 7.1-6.9

We specifically examined the genes that are commonly reported in the scientific literature as being involved in the calcification process and in the formation of the organic matrix of the shell and periostracum. We found that the expression of 60% of the 38 genes involved in the calcification process that were retained by our models showed pH tipping points between 6.9 and 7.1 (Table 2). These genes encode for calcium-binding proteins, Ca^{2+} signaling pathway, amorphous calcium carbonate-binding proteins and ion transmembrane transporters. Most of these genes decreased below the tipping-point (n = 14) while others increased (n = 8). The expression of genes associated with the regulation of the synthesis of the shell organic matrix and the periostracum (n = 11) generally increased with decreasing pH (Table 2). The relationships were loglinear (n = 3) or piecewise (n = 8).

Among these 38 genes, the family of genes that are the most represented are coding for acetylcholine receptors, monocarboxylate transporters and tyrosinase synthesis (Table 2). The expression of four genes coding for acetylcholine receptors decreased below tipping points at pH 6.9-7.0. The expression of five genes coding for monocarboxylate transporters increased with decreasing pH, and four of them showed pH tipping points between 7.3 and 6.6. The expression of four genes associated to tyrosinase synthesis early increased with decreasing pH and three of them showed tipping points between pH 7.4 and 7.1.

Discussion

Here we provide the first reaction norm of juvenile oyster *C. gigas* assessed by combining macro-physiological traits and micro-molecular characteristics. This novel approach applied to juvenile oysters exposed to a wide range of pH conditions revealed

that macro-physiological parameters such as growth, calcification, food intake, and respiration exhibited pH tipping points that coincide with a major reshuffling in membrane lipids and transcriptome that was previously unappreciated, but others like shell parameters seemed uncoupled from global effects (Figure 5). This comprehensive view of the oyster response to pH sheds new light on adaptation capacity of this species to OA. We indeed identify low tipping points for most physiological traits that suggest the species is robust to OA, but reveal sensitivity of shell parameters above the tipping points that potentially impact animal fitness. We therefore determine the true sensitivity of oyster to pH and identify the most relevant and sensitive response variables.

We first identify a global tolerance threshold for juvenile *C. gigas* at pH 6.9-7.3, corresponding to the tipping points identified for the majority of the examined parameters. In line with this, several studies based on IPCC scenario assumed the existence of tipping points below pH 7.5-7.4 for growth, calcification, acid-base equilibrium, and reproduction in oysters and mussels (Boulais et al., 2017; Fitzer et al., 2014; Lannig et al., 2010). Our results are also in agreement with previous studies showing that there are no significant changes in growth, respiration, mortality, metabolic rate, ion regulation, energy reserves, gene expression and fatty acid profile in juveniles and adults of *C. gigas* for pH values above 7.3. (Clark et al., 2013; Lannig et al., 2010; Lemasson et al., 2018; Timmins-Schiffman et al., 2014; Wang et al., 2020). Below tipping points, growth, calcification, respiration and feeding rate decreased markedly, likely reflecting increasing maintenance cost up until reaching critical points that are representative of metabolic depression (Michaelidis et al., 2005; Sokolova, 2021). It is noteworthy that longer exposure time might have revealed an impact of the pH on survival or reproduction, two important parameters for fitness. Survival should be compromised

546 below the tipping point as the animal shift to metabolic depression, i.e., a short-term
547 survival strategy (Michaelidis et al., 2005).

548 The tipping points we determined at pH 7.3-6.9 (pCO_2 ~2600-8200 µatm) are well
549 below IPCC projections for 2100 in open ocean waters (pH=7.8 according to scenario
550 RCP 8.5 IPCC, 2019). However, acidification events with pH values as low as 7.4-7.0
551 (pCO_2 > 3000 µatm) currently occur transiently in estuarine ecosystems in relation to
552 eutrophication and hypoxia (Frankignoulle et al., 1996; Melzner et al., 2013; Proum et
553 al., 2017; Wallace et al., 2014) and may explain why the physiological tipping point of
554 oysters is so low. These acidification events are expected to become increasingly frequent
555 and intense in the future (IPCC, 2019), such that the physiological tipping points defined
556 here for juvenile oysters may be reached.

557 This point outs the importance of tipping point for coastal management and
558 conservation in a changing world. Tipping-point is valid for a whole population
559 regardless of habitat. Here we used juveniles that originate from a large genetic pool and
560 *C. gigas* is a weakly genetically-structured species (Meistertzheim et al., 2013). However,
561 it was recently shown that some wild and domesticated oysters populations vary in their
562 adaptive response to OA (Durland et al., 2021). We therefore need to verify that pH
563 tipping points defined in our study are valid in genetically differentiated populations
564 before integrating them in biogeographic models of species distribution. Finally, tipping
565 point is a single value that reflects susceptibility to stressors that is easily communicable
566 to end-users and society (Bednaršek et al., 2019, 2021).

567 We show here that shell parameters, i.e. thickness, weight and length, were altered
568 as soon as pH decreased from ambient levels, as already reported for many shellfish
569 species (Byrne & Fitzer, 2019). Shell thickness is generally related to shell strength and
570 therefore with protection against predation and resistance to mechanical stress related to

wave exposure and aquaculture processes. Thus, moderate acidification increases predation risk of young *C. gigas* through reduction of shell strength (Wright et al., 2018). We also find that respiration rate first increased when pH decreased, suggesting that metabolism was readily impacted. However, body condition (dry flesh weight) and energy reserves (TAG-ST and carbohydrate, Supplementary Figure 4) were not affected by pH, likely because oysters were fed *ad libitum* (Leung et al., 2019; Thomsen et al., 2013). Finally, we report here a linear increase in the expression level of genes related to GTPase activity and GTP binding, which are characteristics of stress response in *Crassostrea* spp. (Yan et al., 2018). Overall, these changes suggest that longer exposure to moderate acidification (above tipping point) could impair overall oyster fitness.

We further show that this reduction in shell parameters was not related to metabolic depression or to changes in net calcification or global gene expression. In contrast, a recent meta-analysis on *C. gigas* suggests that OA induces a reduction in shell thickness that is related to an overall transcriptional change inducing metabolic depression and alteration of calcification rate (Ducker & Falkenberg, 2020). Here we revisit these assumptions and find in agreement with other prior studies that no metabolic disruptions occurred while shell strength and thickness decreased at pH 7.3-7.7 (Timmins-Schiffman et al., 2014; Wright et al., 2018).

Concomitantly, a delamination of the periostracum, the organic coat covering the shell, may have occurred at pH levels above the tipping point, probably altering shell protection. This was supported by an increase in shell bleaching (not measured) and expression of four genes coding for tyrosinase-like proteins. Tyrosinases are involved in periostracum synthesis and the increase in expression of their related genes is often considered as a mechanism to limit the damage to the periostracum and the corrosion of the shell in reaction to OA (Hüning et al., 2013). Delamination of the periostracum due

596 to moderate OA was frequently associated with alteration of shell properties such as
597 weakening and thinning (Alma et al., 2020; Auzoux-Bordenave et al., 2019; Bressan et
598 al., 2014; Coleman et al., 2014; Peck et al., 2016, 2018; Zhao et al., 2020). Our results
599 agree with the idea that OA is more a dissolution problem than a biomineralization
600 problem (Rajan et al., 2021).

601 This investigation of tipping points at the micro-scale also provides new insights
602 on the physiological response of oysters to OA. For the first time, we find a major
603 remodeling of membrane lipids in response to OA and observed a tipping point at pH 6.9.
604 This remodeling consisted of decreasing the long chain PUFA DHA (22:6n-3) that is
605 essential for growth and survival (Knauer & Southgate, 1999; Langdon & Waldock,
606 1981), at the benefit of eicosanoid precursors (ARA, 20:4n-6 and EPA, 20:5n-3) involved
607 in the stress response (Delaporte et al., 2003). Since membrane fatty acid composition
608 influences the activity of transmembrane proteins involved in ion transport (Hazel &
609 Williams, 1990; Hochachka & Somero, 2002), it could also have been related to
610 regulation of acid-base homeostasis and perhaps calcification under OA.

611 In line with this, we find an overall decrease in expression of genes related to
612 cation transmembrane transport below tipping points at pH 6.9-7.2 that can be related to
613 alteration of calcification and acid-base homeostasis (Zhao et al., 2020). Concomitantly,
614 we observe an overall decrease in the expression of genes coding for proteins involved
615 in the regulation of calcification though calcium signaling pathway, calcium homeostasis,
616 calmodulin signaling pathway and regulation of calcium carbonate crystal growth (Feng
617 et al., 2017; Wang et al., 2017; Zhao et al., 2020).

618 In our analysis, we also identify families of genes that must play an important role
619 in oyster response to OA. Among these genes, we identify four genes coding for
620 acetylcholine receptors that are known for regulating and ordering the formation of the

shell micro-structure (Feng et al., 2017). We also find five monocarboxylate transporters coding genes, members of a family of proteins that act as co-transporters of protons H^+, that may be involved in the regulation of acid-base homeostasis and calcification process (Tresguerres et al., 2020; Wang et al., 2020). These proteins also co-transport monocarboxylates such as lactate or pyruvate and were reported to be involved in the stress response of oysters through induction of anaerobiosis under metabolic depression (Ertl et al., 2019).

In conclusion, we show that juvenile *C. gigas* have a broad tolerance to ocean acidification, exhibiting tipping points around pH 7.3-6.9 for most parameters (Figure 5). Nonetheless, we observe that shell parameters change as soon as pH drops, well before tipping points are reached, suggesting animal fitness is likely to be affected. This thus raises concerns about the future of natural and farmed oyster populations in a high-CO_2 world. This new framework for identification of tolerance threshold in organisms represents a breakthrough in the field of global change research. It was made possible by (1) combining reaction norm assessment and thorough molecular and biochemical analyses of animal responses, and (2) developing a procedure to analyze and synthesize omics data measured over an environmental range.

We believe that such an integrative and holistic approach could now be applied to other organisms and integrate intra-specific variation, life-stages, generations, and other stressors such as temperature, nutrition, pollutants or oxygen levels. Although this approach requires significant financial resources, it allows to determine the true sensitivity of a species to a stressor and to identify the most relevant and sensitive response variables to study in the future.

Acknowledgments

We are grateful for K. Lugue, J. Veillet, C. Quéré, V. Le Roy and I. Queau for their participation to data recording and the Ifremer staff for their involvement in oyster and algae production. We thank J. Thebault and E. Dabass for their advices in shell analysis. We are also grateful for G. Le Moullac for project conception and funding. This work was funded by the Ocean Acidification Program of the French Foundation for Research on Biodiversity (FRB - www.fondationbiodiversite.fr) and the French Ministère de la transition écologique.

Author contributions

ML, CDP, and FP designed and conducted the experiment. All authors analyzed the data. ML performed statistics. ML and FP wrote the first draft of the document and all authors contributed and accepted it. FP and JL obtained the funding. This work is part of the PhD thesis of ML.

Data availability

RNA-seq data have been made available through the SRA database (BioProject accession number PRJNA735889). Other data analyzed during this study are included in this published article and its supplementary information files or available through the SEANOE database (https://doi.org/10.17882/83294). Complementary information is available from the corresponding authors on reasonable request.

Competing interests

The authors declare no competing interests.

Bibliography

Alma, L., Kram, K. E., Holtgrieve, G. W., Barbarino, A., Fiamengo, C. J., & Padilla-Gamiño, J. L. (2020). Ocean acidification and warming effects on the physiology, skeletal properties, and microbiome of the purple-hinge rock scallop.

Comparative Biochemistry and Physiology Part A: Molecular & Integrative Physiology, *240*, 110579. https://doi.org/10.1016/j.cbpa.2019.110579

Aminot, A., & Kérouel, R. (2007). *Dosage automatique des nutriments dans les eaux marines* (MEDD, Editions Quae). Ifremer. https://www.quae.com/produit/924/9782759200238/dosage-automatique-des-nutriments-dans-les-eaux-marines

Auzoux-Bordenave, S., Wessel, N., Badou, A., Martin, S., M'Zoudi, S., Avignon, S., Roussel, S., Huchette, S., & Dubois, P. (2019). Ocean acidification impacts growth and shell mineralization in juvenile abalone (Haliotis tuberculata). *Marine Biology*, *167*(1), 11. https://doi.org/10.1007/s00227-019-3623-0

Bayne, B. L. (2017). *Biology of Oysters* (Vol. 41). Academic Press.

Bednaršek, N., Calosi, P., Feely, R. A., Ambrose, R., Byrne, M., Chan, K. Y. K., Dupont, S., Padilla-Gamiño, J. L., Spicer, J. I., Kessouri, F., Roethler, M., Sutula, M., & Weisberg, S. B. (2021). Synthesis of Thresholds of Ocean Acidification Impacts on Echinoderms. *Frontiers in Marine Science*, *8*. https://doi.org/10.3389/fmars.2021.602601

Bednaršek, N., Feely, R. A., Howes, E. L., Hunt, B. P. V., Kessouri, F., León, P., Lischka, S., Maas, A. E., McLaughlin, K., Nezlin, N. P., Sutula, M., & Weisberg, S. B. (2019). Systematic Review and Meta-Analysis Toward Synthesis of Thresholds of Ocean Acidification Impacts on Calcifying Pteropods and Interactions With Warming. *Frontiers in Marine Science*, *6*. https://doi.org/10.3389/fmars.2019.00227

Boulais, M., Chenevert, K. J., Demey, A. T., Darrow, E. S., Robison, M. R., Roberts, J. P., & Volety, A. (2017). Oyster reproduction is compromised by acidification

694 experienced seasonally in coastal regions. *Scientific Reports*, *7*(1), 13276.
695 https://doi.org/10.1038/s41598-017-13480-3
696 Bressan, M., Chinellato, A., Munari, M., Matozzo, V., Manci, A., Marčeta, T., Finos, L.,
697 Moro, I., Pastore, P., Badocco, D., & Marin, M. G. (2014). Does seawater
698 acidification affect survival, growth and shell integrity in bivalve juveniles?
699 *Marine Environmental Research*, *99*, 136–148.
700 https://doi.org/10.1016/j.marenvres.2014.04.009
701 Browman, H. I. (2017). Towards a broader perspective on ocean acidification research.
702 *ICES Journal of Marine Science*, *74*(4), 889–894.
703 https://doi.org/10.1093/icesjms/fsx073
704 Byrne, M., & Fitzer, S. (2019). The impact of environmental acidification on the
705 microstructure and mechanical integrity of marine invertebrate skeletons.
706 *Conservation Physiology*, *7*(1), 62–82. https://doi.org/10.1093/conphys/coz062
707 Caldeira, K., & Wickett, M. E. (2003). Anthropogenic carbon and ocean pH. *Nature*,
708 *425*(6956), 365–365. https://doi.org/10.1038/425365a
709 Clark, M. S., Thorne, M. A. S., Amaral, A., Vieira, F., Batista, F. M., Reis, J., & Power,
710 D. M. (2013). Identification of molecular and physiological responses to chronic
711 environmental challenge in an invasive species: The Pacific oyster, Crassostrea
712 gigas. *Ecology and Evolution*, *3*(10), 3283–3297.
713 https://doi.org/10.1002/ece3.719
714 Coleman, D., Byrne, M., & Davis, A. (2014). Molluscs on acid: Gastropod shell repair
715 and strength in acidifying oceans. *Marine Ecology Progress Series*, *509*, 203–211.
716 https://doi.org/10.3354/meps10887
717 Comeau, S., Edmunds, P. J., Spindel, N. B., & Carpenter, R. C. (2013). The responses of
718 eight coral reef calcifiers to increasing partial pressure of CO2 do not exhibit a

719 tipping point. *Limnology and Oceanography*, *58*(1), 388–398.
720 https://doi.org/10.4319/lo.2013.58.1.0388
721 Cyronak, T., Schulz, K. G., & Jokiel, P. L. (2016). The Omega myth: What really drives
722 lower calcification rates in an acidifying ocean. *ICES Journal of Marine Science*,
723 *73*(3), 558–562. https://doi.org/10.1093/icesjms/fsv075
724 Delaporte, M., Soudant, P., Moal, J., Lambert, C., Quéré, C., Miner, P., Choquet, G.,
725 Paillard, C., & Samain, J.-F. (2003). Effect of a mono-specific algal diet on
726 immune functions in two bivalve species—Crassostrea gigas and Ruditapes
727 philippinarum. *Journal of Experimental Biology*, *206*(17), 3053–3064.
728 https://doi.org/10.1242/jeb.00518
729 Dickson, A. G., Sabine, C. L., & Christian, J. R. (2007). *Guide to Best Practices for*
730 *Ocean CO2 Measurements* (PICES Special Publication 3). North Pacific Marine
731 Science Organization. https://www.ncei.noaa.gov/access/ocean-carbon-data-
732 system/oceans/Handbook_2007.html
733 Dineshram, R., Quan, Q., Sharma, R., Chandramouli, K., Yalamanchili, H. K., Chu, I., &
734 Thiyagarajan, V. (2015). Comparative and quantitative proteomics reveal the
735 adaptive strategies of oyster larvae to ocean acidification. *Proteomics*, *15*(23–24),
736 4120–4134. https://doi.org/10.1002/pmic.201500198
737 Dorey, N., Lançon, P., Thorndyke, M., & Dupont, S. (2013). Assessing physiological
738 tipping point of sea urchin larvae exposed to a broad range of pH. *Global Change*
739 *Biology*, *19*(11), 3355–3367. https://doi.org/10.1111/gcb.12276
740 DuBois, Michel., Gilles, K. A., Hamilton, J. K., Rebers, P. A., & Smith, Fred. (1956).
741 Colorimetric Method for Determination of Sugars and Related Substances.
742 *Analytical Chemistry*, *28*(3), 350–356. https://doi.org/10.1021/ac60111a017

743 Ducker, J., & Falkenberg, L. J. (2020). How the Pacific Oyster Responds to Ocean
744 Acidification: Development and Application of a Meta-Analysis Based Adverse
745 Outcome Pathway. *Frontiers in Marine Science*, *7*(7), 398–408.
746 Durland, E., De Wit, P., Meyer, E., & Langdon, C. (2021). Larval development in the
747 Pacific oyster and the impacts of ocean acidification: Differential genetic effects
748 in wild and domesticated stocks. *Evolutionary Applications*, *14*(9), 2258–2272.
749 https://doi.org/10.1111/eva.13289
750 Ertl, N. G., O'Connor, W. A., & Elizur, A. (2019). Molecular effects of a variable
751 environment on Sydney rock oysters, Saccostrea glomerata: Thermal and low
752 salinity stress, and their synergistic effect. *Marine Genomics*, *43*, 19–32.
753 https://doi.org/10.1016/j.margen.2018.10.003
754 FAO. (2020). *The State of World Fisheries and Aquaculture 2020. In brief. Sustainability*
755 *in action.* Rome.
756 Feng, D., Li, Q., Yu, H., Kong, L., & Du, S. (2017). Identification of conserved proteins
757 from diverse shell matrix proteome in Crassostrea gigas: Characterization of
758 genetic bases regulating shell formation. *Scientific Reports*, *7*(1), 45–54.
759 https://doi.org/10.1038/srep45754
760 Fitzer, S. C., Phoenix, V. R., Cusack, M., & Kamenos, N. A. (2014). Ocean acidification
761 impacts mussel control on biomineralisation. *Scientific Reports*, *4*(1), 6218.
762 https://doi.org/10.1038/srep06218
763 Frankignoulle, M., Bourge, I., & Wollast, R. (1996). Atmospheric CO2 fluxes in a highly
764 polluted estuary (the Scheldt). *Limnology and Oceanography*, *41*(2), 365–369.
765 https://doi.org/10.4319/lo.1996.41.2.0365
766 Gazeau, F., Alliouane, S., Bock, C., Bramanti, L., López Correa, M., Gentile, M., Hirse,
767 T., Pörtner, H.-O., & Ziveri, P. (2014). Impact of ocean acidification and warming

768 on the Mediterranean mussel (Mytilus galloprovincialis). *Frontiers in Marine*
769 *Science*, *1*, 62. https://doi.org/10.3389/fmars.2014.00062
770 Gazeau, F., Parker, L. M., Comeau, S., Gattuso, J.-P., O'Connor, W. A., Martin, S.,
771 Pörtner, H.-O., & Ross, P. M. (2013). Impacts of ocean acidification on marine
772 shelled molluscs. *Marine Biology*, *160*(8), 2207–2245.
773 https://doi.org/10.1007/s00227-013-2219-3
774 Gazeau, F., Urbini, L., Cox, T. E., Alliouane, S., & Gattuso, J.-P. (2015). Comparison of
775 the alkalinity and calcium anomaly techniques to estimate rates of net
776 calcification. *Marine Ecology Progress Series*, *527*, 1–12.
777 https://doi.org/10.3354/meps11287
778 Hazel, J. R., & Williams, E. (1990). The role of alterations in membrane lipid composition
779 in enabling physiological adaptation of organisms to their physical environment.
780 *Progress in Lipid Research*, *29*(3), 167–227. https://doi.org/10.1016/0163-
781 7827(90)90002-3
782 Hochachka, P. W., & Somero, G. (2002). Biochemical adaptation: Mechanism and
783 process in physiological evolution. *Biochemistry and Molecular Biology*
784 *Education*, *30*(3), 215–216. https://doi.org/10.1002/bmb.2002.494030030071
785 Hulbert, A. J., & Else, P. L. (1999). Membranes as possible pacemakers of metabolism.
786 *Journal of Theoretical Biology*, *199*(3), 257–274.
787 https://doi.org/10.1006/jtbi.1999.0955
788 Hüning, A. K., Melzner, F., Thomsen, J., Gutowska, M. A., Krämer, L., Frickenhaus, S.,
789 Rosenstiel, P., Pörtner, H.-O., Philipp, E. E. R., & Lucassen, M. (2013). Impacts
790 of seawater acidification on mantle gene expression patterns of the Baltic Sea blue
791 mussel: Implications for shell formation and energy metabolism. *Marine Biology*,
792 *160*(8), 1845–1861.

IPCC. (2019). *IPCC Special Report on the Ocean and Cryosphere in a Changing Climate: Vol. (eds Pörtner, H. O. et al.)* (H. O. Pörtner, D. C. Roberts, V. Masson-Delmotte, P. Zhai, M. Tignor, E. Poloczanska, K. Mintenbeck, A. Alegria, M. Nicolai, A. Okem, J. Petzold, B. Rama, & N. M. Weyer, Eds.; H.-O. Pörtner, D.C. Roberts, V. Masson-Delmotte, P. Zhai, M. Tignor, E. Poloczanska, K. Mintenbeck, A. Alegría, M. Nicolai, A. Okem, J. Petzold, B. Rama, N.M. Weyer (eds.)). In. press.

IPCC. (2021). *Climate Change 2021: The Physical Science Basis. Contribution of Working Group I to the Sixth Assessment Report of the Intergovernmental Panel on Climate Change: Vol. (eds Masson-Delmotte, V. P. et al.)*. Cambridge University Press. In Press.

Klopfenstein, D. V., Zhang, L., Pedersen, B. S., Ramírez, F., Warwick Vesztrocy, A., Naldi, A., Mungall, C. J., Yunes, J. M., Botvinnik, O., Weigel, M., Dampier, W., Dessimoz, C., Flick, P., & Tang, H. (2018). GOATOOLS: A Python library for Gene Ontology analyses. *Scientific Reports*, *8*(1), 10872. https://doi.org/10.1038/s41598-018-28948-z

Knauer, J., & Southgate, P. C. (1999). A Review of the Nutritional Requirements of Bivalves and the Development of Alternative and Artificial Diets for Bivalve Aquaculture. *Reviews in Fisheries Science*, *7*(3–4), 241–280. https://doi.org/10.1080/10641269908951362

Ko, G. W. K., Dineshram, R., Campanati, C., Chan, V. B. S., Havenhand, J., & Thiyagarajan, V. (2014). Interactive effects of ocean acidification, elevated temperature, and reduced salinity on early-life stages of the pacific oyster. *Environmental Science & Technology*, *48*(17), 10079–10088. https://doi.org/10.1021/es501611u

818 Kroeker, K. J., Kordas, R. L., Crim, R., Hendriks, I. E., Ramajo, L., Singh, G. S., Duarte,
819 C. M., & Gattuso, J.-P. (2013). Impacts of ocean acidification on marine
820 organisms: Quantifying sensitivities and interaction with warming. *Global*
821 *Change Biology*, *19*(6), 1884–1896. https://doi.org/10.1111/gcb.12179
822 Langdon, C. J., & Waldock, M. J. (1981). The effect of algal and artificial diets on the
823 growth and fatty acid composition of Crassostrea gigas Spat. *Journal of the*
824 *Marine Biological Association of the United Kingdom*, *61*(2), 431–448.
825 https://doi.org/10.1017/S0025315400047056
826 Langfelder, P., & Horvath, S. (2008). WGCNA: An R package for weighted correlation
827 network analysis. *BMC Bioinformatics*, *9*, 559. https://doi.org/10.1186/1471-
828 2105-9-559
829 Lannig, G., Eilers, S., Pörtner, H. O., Sokolova, I. M., & Bock, C. (2010). Impact of
830 Ocean Acidification on Energy Metabolism of Oyster, Crassostrea gigas—
831 Changes in Metabolic Pathways and Thermal Response. *Marine Drugs*, *8*(8),
832 2318–2339. https://doi.org/10.3390/md8082318
833 Lee, H.-G., Stumpp, M., Yan, J.-J., Tseng, Y.-C., Heinzel, S., & Hu, M. Y.-A. (2019).
834 Tipping points of gastric pH regulation and energetics in the sea urchin larva
835 exposed to CO2 -induced seawater acidification. *Comparative Biochemistry and*
836 *Physiology Part A: Molecular & Integrative Physiology*, *234*, 87–97.
837 https://doi.org/10.1016/j.cbpa.2019.04.018
838 Lemasson, A. J., Hall-Spencer, J. M., Fletcher, S., Provstgaard-Morys, S., & Knights, A.
839 M. (2018). Indications of future performance of native and non-native adult
840 oysters under acidification and warming. *Marine Environmental Research*, *142*,
841 178–189. https://doi.org/10.1016/j.marenvres.2018.10.003

842 Leung, J. Y. S., Doubleday, Z. A., Nagelkerken, I., Chen, Y., Xie, Z., & Connell, S. D.
843 (2019). How calorie-rich food could help marine calcifiers in a CO2-rich future.
844 *Proceedings of the Royal Society B: Biological Sciences*, *286*(1906), 20190757.
845 https://doi.org/10.1098/rspb.2019.0757
846 Matz, M. V. (2018). Fantastic Beasts and How To Sequence Them: Ecological Genomics
847 for Obscure Model Organisms. *Trends in Genetics: TIG*, *34*(2), 121–132.
848 https://doi.org/10.1016/j.tig.2017.11.002
849 Meistertzheim, A.-L., Arnaud-Haond, S., Boudry, P., & Thébault, M.-T. (2013). Genetic
850 structure of wild European populations of the invasive Pacific oyster Crassostrea
851 gigas due to aquaculture practices. *Marine Biology*, *160*(2), 453–463.
852 https://doi.org/10.1007/s00227-012-2102-7
853 Melzner, F., Thomsen, J., Koeve, W., Oschlies, A., Gutowska, M. A., Bange, H. W.,
854 Hansen, H. P., & Körtzinger, A. (2013). Future ocean acidification will be
855 amplified by hypoxia in coastal habitats. *Marine Biology*, *160*(8), 1875–1888.
856 https://doi.org/10.1007/s00227-012-1954-1
857 Michaelidis, B., Ouzounis, C., Paleras, A., & Pörtner, H. (2005). *Effects of long-term*
858 *moderate hypercapnia on acid-base balance and growth rate in marine mussels*
859 *(Mytilus galloprovincialis)*. *293*, 109–118. https://doi.org/10.3354/MEPS293109
860 Orr, J. C., Fabry, V. J., Aumont, O., Bopp, L., Doney, S. C., Feely, R. A., Gnanadesikan,
861 A., Gruber, N., Ishida, A., Joos, F., Key, R. M., Lindsay, K., Maier-Reimer, E.,
862 Matear, R., Monfray, P., Mouchet, A., Najjar, R. G., Plattner, G.-K., Rodgers, K.
863 B., … Yool, A. (2005). Anthropogenic ocean acidification over the twenty-first
864 century and its impact on calcifying organisms. *Nature*, *437*(7059), 681–686.
865 https://doi.org/10.1038/nature04095

Peck, V. L., Oakes, R. L., Harper, E. M., Manno, C., & Tarling, G. A. (2018). Pteropods counter mechanical damage and dissolution through extensive shell repair. *Nature Communications*, *9*(1), 264. https://doi.org/10.1038/s41467-017-02692-w

Peck, V. L., Tarling, G. A., Manno, C., Harper, E. M., & Tynan, E. (2016). Outer organic layer and internal repair mechanism protects pteropod Limacina helicina from ocean acidification. *Deep Sea Research Part II: Topical Studies in Oceanography*, *127*, 41–52. https://doi.org/10.1016/j.dsr2.2015.12.005

Peñaloza, C., Gutierrez, A. P., Eöry, L., Wang, S., Guo, X., Archibald, A. L., Bean, T. P., & Houston, R. D. (2021). A chromosome-level genome assembly for the Pacific oyster Crassostrea gigas. *GigaScience*, *10*(3). https://doi.org/10.1093/gigascience/giab020

Petton, B., Boudry, P., Alunno-Bruscia, M., & Pernet, F. (2015). Factors influencing disease-induced mortality of Pacific oysters Crassostrea gigas. *Aquaculture Environment Interactions*, *6*(3), 205–222. https://doi.org/10.3354/aei00125

Proum, S., Harley, C. D., Steele, M., & Marshall, D. J. (2017). Aerobic and behavioral flexibility allow estuarine gastropods to flourish in rapidly changing and extreme pH conditions. *Marine Biology*, *164*(5), 97. https://doi.org/10.1007/s00227-017-3124-y

Rajan, K. C., Meng, Y., Yu, Z., Roberts, S. B., & Vengatesen, T. (2021). Oyster biomineralization under ocean acidification: From genes to shell. *Global Change Biology*, *27*(16), 3779–3797. https://doi.org/10.1111/gcb.15675

Rico-Villa, B., Pouvreau, S., & Robert, R. (2009). Influence of food density and temperature on ingestion, growth and settlement of Pacific oyster larvae, Crassostrea gigas. *Aquaculture*, *287*(3), 395–401. https://doi.org/10.1016/j.aquaculture.2008.10.054

Schneider, C. A., Rasband, W. S., & Eliceiri, K. W. (2012). NIH Image to ImageJ: 25 years of image analysis. *Nature Methods*, *9*(7), 671–675. https://doi.org/10.1038/nmeth.2089

Smith, S. V., & Key, G. S. (1975). Carbon dioxide and metabolism in marine environments. *Limnology and Oceanography*, *20*(3), 493–495. https://doi.org/10.4319/lo.1975.20.3.0493

Sokolova, I. M. (2021). Bioenergetics in environmental adaptation and stress tolerance of aquatic ectotherms: Linking physiology and ecology in a multi-stressor landscape. *Journal of Experimental Biology*, *224*(Suppl 1). https://doi.org/10.1242/jeb.236802

Strader, M. E., Wong, J. M., & Hofmann, G. E. (2020). Ocean acidification promotes broad transcriptomic responses in marine metazoans: A literature survey. *Frontiers in Zoology*, *17*(1), 7–30. https://doi.org/10.1186/s12983-020-0350-9

Thomsen, J., Casties, I., Pansch, C., Körtzinger, A., & Melzner, F. (2013). Food availability outweighs ocean acidification effects in juvenile Mytilus edulis: Laboratory and field experiments. *Global Change Biology*, *19*(4), 1017–1027. https://doi.org/10.1111/gcb.12109

Timmins-Schiffman, E., Coffey, W. D., Hua, W., Nunn, B. L., Dickinson, G. H., & Roberts, S. B. (2014). Shotgun proteomics reveals physiological response to ocean acidification in Crassostrea gigas. *BMC Genomics*, *15*(1), 951. https://doi.org/10.1186/1471-2164-15-951

Tresguerres, M., Clifford, A. M., Harter, T. S., Roa, J. N., Thies, A. B., Yee, D. P., & Brauner, C. J. (2020). Evolutionary links between intra- and extracellular acid–base regulation in fish and other aquatic animals. *Journal of Experimental*

915 *Zoology Part A: Ecological and Integrative Physiology*, *333*(6), 449–465.
916 https://doi.org/10.1002/jez.2367
917 Tresguerres, M., & Hamilton, T. J. (2017). Acid–base physiology, neurobiology and
918 behaviour in relation to CO2-induced ocean acidification. *Journal of*
919 *Experimental Biology*, *220*(12), 2136–2148. https://doi.org/10.1242/jeb.144113
920 Vargas, C. A., Lagos, N. A., Lardies, M. A., Duarte, C., Manríquez, P. H., Aguilera, V.
921 M., Broitman, B., Widdicombe, S., & Dupont, S. (2017). Species-specific
922 responses to ocean acidification should account for local adaptation and adaptive
923 plasticity. *Nature Ecology & Evolution*, *1*(4), 1–7.
924 https://doi.org/10.1038/s41559-017-0084
925 Ventura, A., Schulz, S., & Dupont, S. (2016). Maintained larval growth in mussel larvae
926 exposed to acidified under-saturated seawater. *Scientific Reports*, *6*(1), 23728.
927 https://doi.org/10.1038/srep23728
928 Waldbusser, G. G., & Salisbury, J. E. (2014). Ocean Acidification in the Coastal Zone
929 from an Organism's Perspective: Multiple System Parameters, Frequency
930 Domains, and Habitats. *Annual Review of Marine Science*, *6*(1), 221–247.
931 https://doi.org/10.1146/annurev-marine-121211-172238
932 Wallace, R. B., Baumann, H., Grear, J. S., Aller, R. C., & Gobler, C. J. (2014). Coastal
933 ocean acidification: The other eutrophication problem. *Estuarine, Coastal and*
934 *Shelf Science*, *148*, 1–13. https://doi.org/10.1016/j.ecss.2014.05.027
935 Wang, X., Wang, M., Jia, Z., Song, X., Wang, L., & Song, L. (2017). A shell-formation
936 related carbonic anhydrase in Crassostrea gigas modulates intracellular calcium
937 against CO2 exposure: Implication for impacts of ocean acidification on mollusk
938 calcification. *Aquatic Toxicology*, *189*, 216–228.
939 https://doi.org/10.1016/j.aquatox.2017.06.009

940 Wang, X., Wang, M., Wang, W., Liu, Z., Xu, J., Jia, Z., Chen, H., Qiu, L., Lv, Z., Wang,
941 L., & Song, L. (2020). Transcriptional changes of Pacific oyster Crassostrea gigas
942 reveal essential role of calcium signal pathway in response to CO2-driven
943 acidification. *The Science of the Total Environment*, *741*, 140177.
944 https://doi.org/10.1016/j.scitotenv.2020.140177
945 Wood, S. N. (2001). Minimizing Model Fitting Objectives That Contain Spurious Local
946 Minima by Bootstrap Restarting. *Biometrics*, *57*(1), 240–244.
947 https://doi.org/10.1111/j.0006-341X.2001.00240.x
948 Wright, J. M., Parker, L. M., O'Connor, W. A., Scanes, E., & Ross, P. M. (2018). Ocean
949 acidification affects both the predator and prey to alter interactions between the
950 oyster Crassostrea gigas (Thunberg, 1793) and the whelk Tenguella marginalba
951 (Blainville, 1832). *Marine Biology*, *165*(3), 46. https://doi.org/10.1007/s00227-
952 018-3302-6
953 Yan, L., Li, Y., Wang, Z., Su, J., Yu, R., Yan, X., Ma, P., & Cui, Y. (2018). Stress
954 response to low temperature: Transcriptomic characterization in Crassostrea
955 sikamea × Crassostrea angulata hybrids. *Aquaculture Research*, *49*(10), 3374–
956 3385. https://doi.org/10.1111/are.13801
957 Yarra, T., Blaxter, M., & Clark, M. S. (2021). A Bivalve Biomineralization Toolbox.
958 *Molecular Biology and Evolution*, *38*(9), 4043–4055.
959 https://doi.org/10.1093/molbev/msab153
960 Zhao, X., Han, Y., Chen, B., Xia, B., Qu, K., & Liu, G. (2020). CO2-driven ocean
961 acidification weakens mussel shell defense capacity and induces global molecular
962 compensatory responses. *Chemosphere*, *243*, 125415.
963 https://doi.org/10.1016/j.chemosphere.2019.125415
964

Figure captions

Figure 1. Oysters exposed to 15 pH conditions for 23 d. Five oysters were selected from each condition, and sorted from the smallest to the biggest. Corresponding pH (total scale) and saturation states of seawater with respect to calcite (Ω_{CA}) are shown.

Figure 2. Biometry and physiological rates of oysters as a function of pH (total scale). (a) shell length, (b) net calcification, (c) growth rate in shell length, (d) growth rate in total body weight (TW), (e) respiration rate, (f) ingestion rate, (g) shell weight, (h) dry flesh weight and (i) minimal shell thickness. Data are means ± SD when available. Tipping points and critical points and their 95% confidence intervals are shown in grey and red, respectively. The significance levels of the slopes are presented using symbols (P< 0.001 ***, < 0.01 **, < 0.05 *, < 0.1 ·).

Figure 3. Membrane fatty acid (FA) composition of oysters as a function of pH (total scale). (a) Principal component analysis of polar fatty acid classes for oysters (n = 15 pools of five oysters) exposed to 15 pH levels. Arrows represent fatty acids contributing to more than 5% of the first principal component (PC1). Individuals are colored according to the average pH. Contribution to membrane of the sum of fatty acids that are (b) positively or (c) negatively correlated to PC1 as a function of pH. Tipping points and their 95% confidence intervals are shown in grey. The significance levels of the slopes are presented using symbols (P < 0.001 ***, < 0.01 **, < 0.05 *, < 0.1 ·).

Figure 4. Tipping points of oyster transcriptome. (a-c) Frequency distribution of tipping-point for piecewise linear relationships (left side). Linear and loglinear models (no tipping-point) are under “Lin” name. Genes are grouped into three clusters of genes that co-vary together. The grey line indicates the distribution frequency of all genes irrespective of clusters. Groups of genes which exhibit neighboring tipping points with distribution frequencies > 5% (shown as a dotted line), were grouped together. The

990 segments above the bars indicate the groups of genes on which GO analyses were
991 conducted. In each case, the gene that best represents the cluster according to module
992 membership, gene significance for pH and R^2 is presented as a function of pH as an
993 example (right side). Tipping points and their 95% confidence intervals are shown in
994 grey. The significance levels of the slopes are presented using stars (P <0.001 ***, p<0.01
995 **, p<0.05 *). Gene names are: LOC117690205: monocarboxylate transporter 12-like,
996 LOC105317113: 60S ribosomal protein L10a, LOC105331560: protocadherin Fat 4
997 **Figure 5.** Graphical summary of the reaction norm of juvenile oysters *Crassostrea gigas*
998 over a wide range of pH conditions. Abbreviations: GO, gene ontology term; ARA,
999 arachidonic acid, EPA, ecosapentaenoic acid, DHA, docosahexaenoic acid, NMI, non-
1000 methylene interrupted.

1001

1002 **Figures**

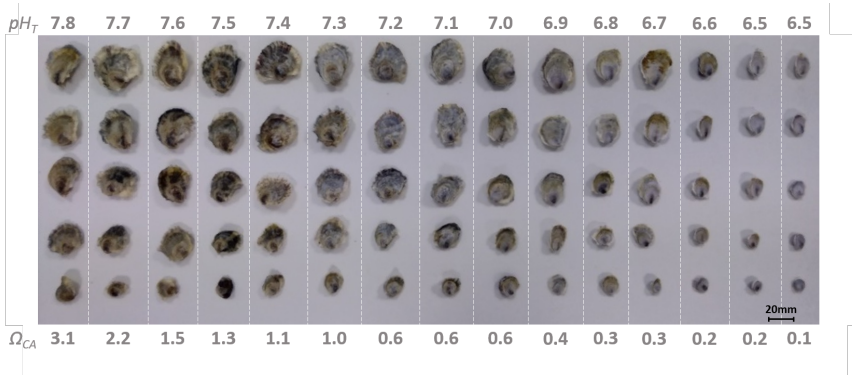

1003

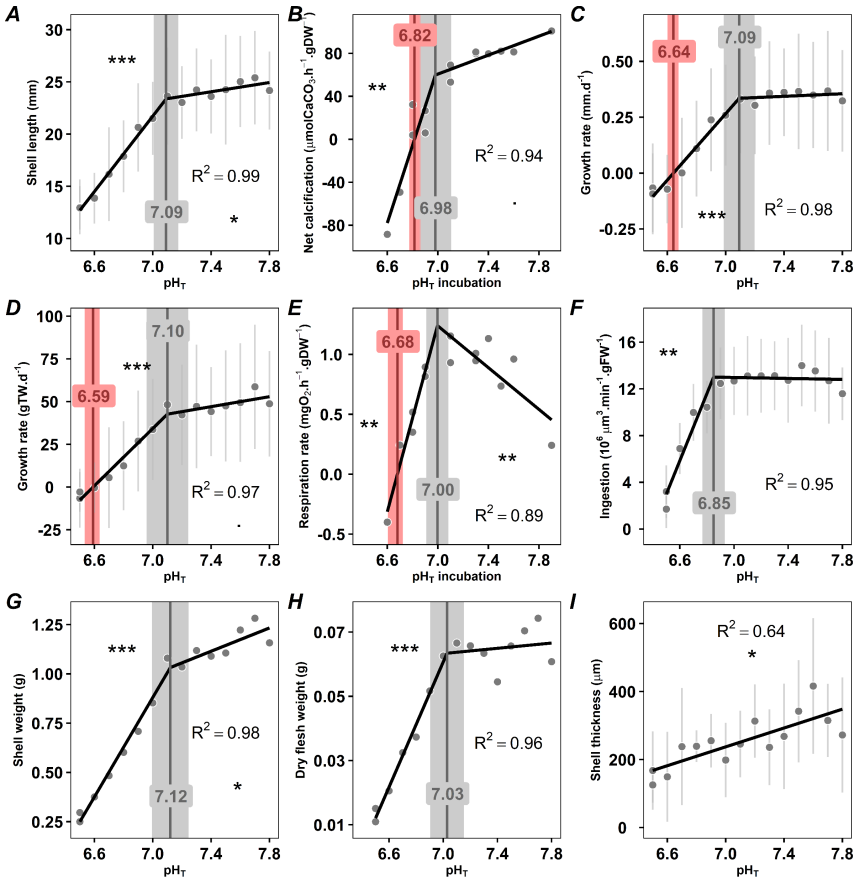
A
Shell length (mm)
***
R² = 0.99
7.09
*
pHT
B
Net calcification (μmolCaCO3.h-1.gDW-1)
6.82
**
R² = 0.94
6.98
pHT incubation
C
Growth rate (mm.d-1)
6.64
7.09
***
R² = 0.98
pHT
D
Growth rate (gTW.d-1)
7.10
***
6.59
R² = 0.97
pHT
E
Respiration rate (mgO2.h-1.gDW-1)
6.68
**
**
7.00
R² = 0.89
pHT incubation
F
Ingestion (10⁶ μm³.min-1.gFW-1)
**
R² = 0.95
6.85
pHT
G
Shell weight (g)
***
R² = 0.98
7.12
*
pHT
H
Dry flesh weight (g)
***
R² = 0.96
7.03
pHT
I
Shell thickness (μm)
R² = 0.64
*
pHT

1004

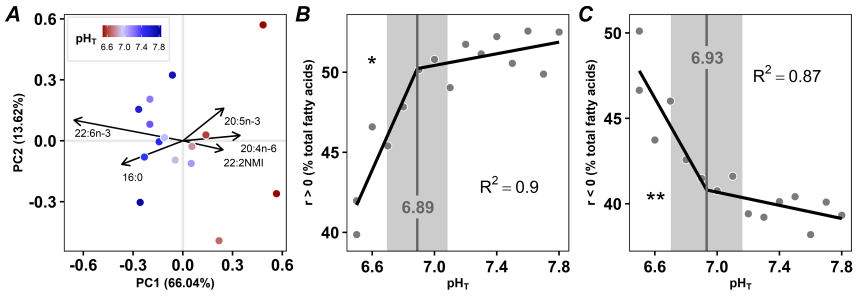
A
B
C
pHT
6.6 7.0 7.4 7.8
22:6n-3
20:5n-3
20:4n-6
22:2NMI
16:0
PC2 (13.62%)
PC1 (66.04%)
r > 0 (% total fatty acids)
r < 0 (% total fatty acids)
pHT
6.89
6.93
R2 = 0.9
R2 = 0.87
*
**

1005

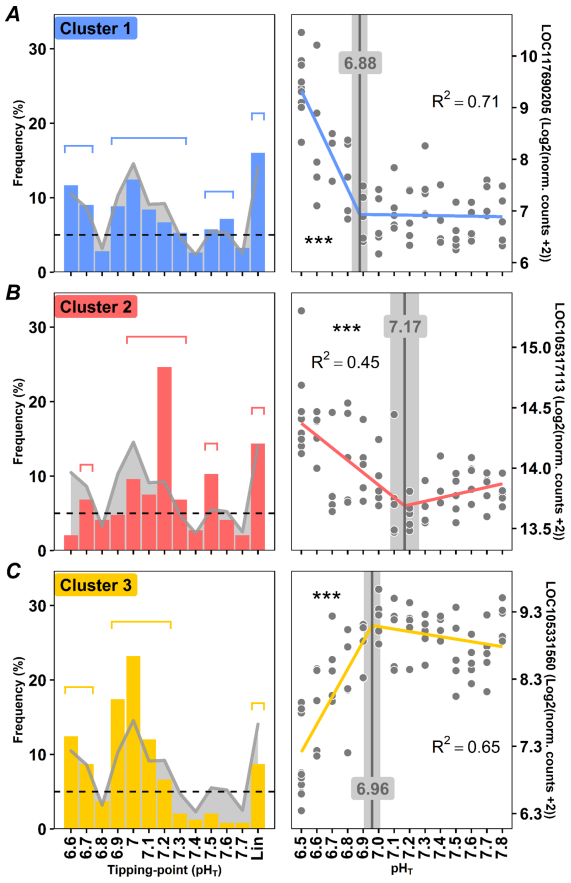
A
Cluster 1
Frequency (%)
6.88
R2 = 0.71
***
LOC117690205 (Log2(norm. counts +2))
B
Cluster 2
***
7.17
R2 = 0.45
LOC105317113 (Log2(norm. counts +2))
C
Cluster 3
***
R2 = 0.65
6.96
LOC105331560 (Log2(norm. counts +2))
Tipping-point (pHT)
pHT

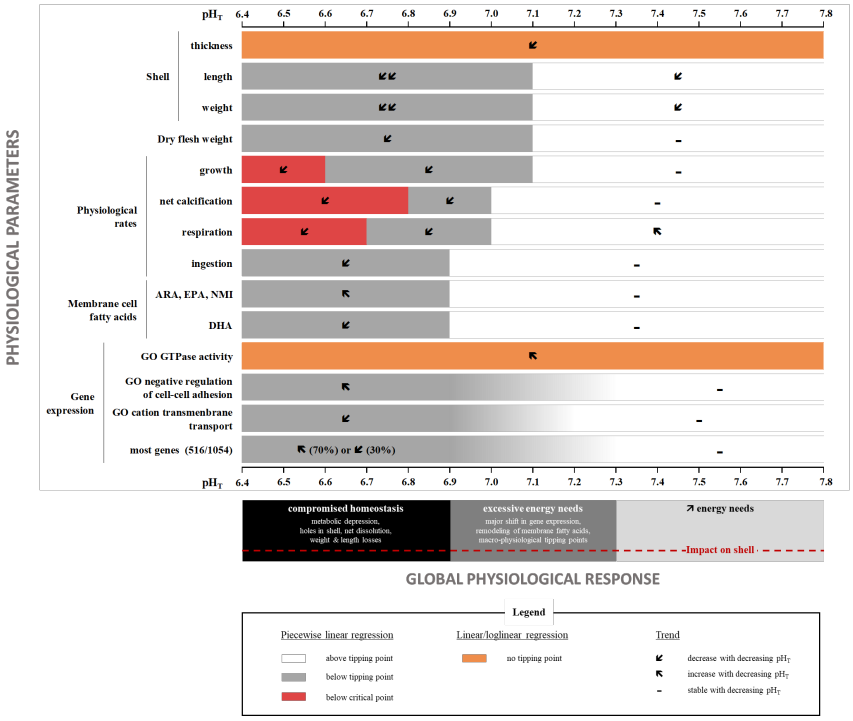

1021

Commented [FP1]: détiller increase energy needs

Table 1 Gene ontology term enrichment and tipping point. Model characteristics, physiological function and gene ontology for each cluster. For each GO term, the P-value of Bonferroni test is displayed using symbols (P < 0.001 ***, < 0.01 **, < 0.05 *, < 0.1 ·). Abbreviations: TP: tipping point

Cluster	Models			Physiological function	Gene Ontology			
	shape of the relationship	*TP range*	*number of genes*		*GO*	*name*	*number of genes*	*p bonferroni*
1	↖←▯	6.9-7.3	283	regulation of RNA-transcription	.....GO:1903506	regulation of nucleic acid-templated transcription	38	**
					.....GO:0006357	regulation of transcription by RNA polymerase II	30	***
				cellular metabolism & macromolecule byosynthesis	.....GO:2000112	regulation of cellular macromolecule biosynthetic process	41	*
					.....GO:0031325	positive regulation of cellular metabolic process	39	*
				cell-cell adhesion	.....GO:0022408	negative regulation of cell-cell adhesion	8	•▯
	↖▯	n.a.	96	GTP metabolism	.....GO:0003924	GTPase activity	8	**
					.....GO:0005525	GTP binding	9	*
				ribonucleotide metabolism	.....GO:0032561	guanyl ribonucleotide binding	9	•▯
					.....GO:0032550	purine ribonucleoside binding	9	•▯
2	↖←▯	7.0-7.3	62	ribosome synthesis / ribosomal subunit assembly	.....GO:0000027	ribosomal large subunit assembly	4	**
					.....GO:0022625	cytosolic large ribosomal subunit	10	***
					.....GO:0022627	cytosolic small ribosomal subunit	6	***
					.....GO:0022618	ribonucleoprotein complex assembly	6	*
				RNA-binding	.....GO:1990932	5.8S rRNA binding	3	***
					.....GO:0019843	rRNA binding	8	***
					.....GO:0003729	mRNA binding	6	*
				translation	.....GO:0002181	cytoplasmic translation	8	***

				protein & amino acids synthesis	.....GO:0043604	amide biosynthetic process	25	***
					.....GO:0043043	peptide biosynthetic process	25	***
				ribosome synthesis / ribosomal subunit assembly	.....GO:0022627	cytosolic small ribosomal subunit	3	**
					.....GO:0022625	cytosolic large ribosomal subunit	6	***
	↖	n.a.	25	translation	.....GO:0006412	translation	10	***
				RNA processing	.....GO:0006364	rRNA processing	4	•
				protein & amino acids synthesis	.....GO:0043043	peptide biosynthetic process	10	***
					.....GO:0043604	amide biosynthetic process	11	***
3					....GO:0006811	ion transport	19	**
	↙←	6.9-7.2	150	ion transport	....GO:0022890	inorganic cation transmembrane transporter activity	14	*
					....GO:0008324	cation transmembrane transporter activity	14	•

1026

1027

Table 2 Tipping points of genes related to calcification and production of the shell organic matrix. Model characteristics and physiological function are reported for each gene. The slope inclination is displayed using arrows only if it is significant according to Student t tests ($P < 0.05$). Abbreviations: TP: tipping point, CBP*: calcium-binding proteins,* ACCBP: *amorphous calcium carbonate-binding proteins*, SMP: *shell matrix proteins.*

Physiological function		**Model**					**Gene**	
		Model	*TP*	*Slope before TP*	*Slope after TP*	R^2	*Cluster*	*Name*
Calcification	*Ion transport*	piecewise	6.6±0.1	↖	n.s.	0.33	1	sodium-dependent phosphate transport protein 2B
			6.6±0.0	↖	n.s.	0.37	1	monocarboxylate transporter 5
	CBP		6.6±0.0	↖	n.s.	0.20	1	fibrillin-2-like
			6.6±0.0	↙	n.s.	0.48	3	EF-hand Ca-binding domain-containing protein 6
	Ca^{2+} signaling pathway		6.7±0.2	n.s.	↖	0.20	2	neurocalcin-delta
	CBP		6.7±0.1	↙	n.s.	0.32	3	ankyrin repeat and EF-hand domain-containing protein 1
	Ca^{2+} signaling pathway		6.8±0.1	↙	n.s.	0.40	3	polycystin-2
			6.9±0.3	n.s.	↖	0.09	1	neurocalcin-like protein
	Ion transport		6.9±0.1	↖	n.s.	0.71	1	monocarboxylate transporter 12-like
	CBP		6.9±0.1	↙	n.s.	0.17	3	D-galactoside-specific lectin
			6.9±0.1	↙	n.s.	0.31	3	sarcoplasmic calcium-binding protein
			6.9±0.1	↙	n.s.	0.42	3	calmodulin-like protein 12
	Ion transport		6.9±0.1	↙	↙	0.45	3	sodium/calcium exchanger 3
	ACCBP		6.9±0.1	↙	n.s.	0.49	3	neuronal acetylcholine receptor subunit alpha-6
			6.9±0.1	↙	n.s.	0.36	3	acetylcholine receptor subunit beta
			6.9±0.1	↙	n.s.	0.31	3	neuronal acetylcholine receptor subunit alpha-3
	Ca^{2+} signaling pathway		7.0±0.2	↖	n.s.	0.17	1	metabotropic glutamate receptor 5
	Signaling pathway		7.0±0.2	↖	n.s.	0.30	1	toll-like receptor 4
	Ion transport		7.0±0.2	n.s.	↖	0.19	1	G protein-activated inward rectifier potassium channel 2
			7.0±0.4	n.s.	↖	0.15	1	monocarboxylate transporter 9
			7.0±0.1	↙	n.s.	0.29	3	organic cation transporter protein
			7.0±0.1	↙	n.s.	0.32	3	small conductance calcium-activated potassium channel protein 2
			7.0±0.1	↙	n.s.	0.24	3	sodium/glucose cotransporter 4

	Ca^{2+} signaling pathway		7.0±0.1	↙	n.s.	0.65	3	protocadherin FAT 4
	ACCBP		7.0±0.1	↙	n.s.	0.43	3	acetylcholine receptor subunit beta-type unc-29
	CBP		7.1±0.3	↖	n.s.	0.28	1	neurogenic locus notch homolog protein 1
	Ca^{2+} signaling pathway		7.1±0.2	↖	n.s.	0.26	1	protocadherin gamma-A4
	CBP		7.1±0.1	↙	↙	0.42	3	delta-like protein 4 / delta-like protein C
	Ion transport		7.1±0.1	↙	n.s.	0.28	3	calcium-activated potassium channel slowpoke
	Ca^{2+} signaling pathway		7.2±0.1	↖	n.s.	0.18	1	protocadherin-11 X-linked
			7.2±0.2	↙	n.s.	0.14	3	cadherin-87A
	Ion transport		7.3±0.2	↖	n.s.	0.20	1	monocarboxylate transporter 12-like
	CBP		7.4±0.1	↖	n.s.	0.29	1	calmodulin-A
	Ca^{2+} signaling pathway		7.5±0.1	↖	n.s.	0.21	1	protocadherin gamma-B1
	Ion transport		7.6±0.1	↖	↖	0.33	1	potassium channel GORK
		loglinear	n.a.	↖	n.a.	0.42	1	monocarboxylate transporter 9-like
	CBP		n.a.	↙	n.a.	0.25	3	fibrillin-1
Shell organic matrix & periostracum	*SMP*	piecewise	6.6±0.0	↖	↖	0.66	1	asparagine-rich protein
			7.0±0.1	↖	n.s.	0.21	1	perlucin-like protein
	SMP, periostracum formation		7.0±0.1	↙	n.s.	0.37	3	putative tyrosinase-like protein tyr-1
			7.1±0.2	↖	n.s.	0.20	1	tyrosinase-like protein 2
			7.4±0.2	↖	n.s.	0.24	1	tyrosinase-like protein 2
			7.4±0.2	↖	n.s.	0.30	1	tyrosinase-like protein 2
	SMP, carbonic anhydrase		7.5±0.2	↖	n.s.	0.19	1	nacrein-like protein F2
			7.5±0.2	↖	n.s.	0.25	1	nacrein-like protein / carbonic anhydrase 6
	SMP	loglinear	n.a.	↙	n.a.	0.23	3	leucine-rich repeat and fibronectin type-III domain-containing protein 5-like
	SMP, periostracum formation		n.a.	↖	n.a.	0.43	1	tyrosinase-like protein 1
	SMP		n.a.	↖	n.a.	0.28	1	circumsporozoite protein-like

1034

Supplementary information

Revisiting tolerance to ocean acidification: insights from a new framework combining physiological and molecular tipping points of Pacific oyster

Mathieu Lutier[1,*], Carole Di Poi[1], Frédéric Gazeau[2], Alexis Appolis[1], Jérémy Le Luyer[3], Fabrice Pernet[1,*]

[1] LEMAR UMR6539, CNRS/UBO/IRD/Ifremer, ZI pointe du diable, CS 10070, F-29280 Plouzané, France.

[2]LOV UMR7093, Sorbonne Université, CNRS, Laboratoire d'Océanographie de Villefranche, Villefranche-sur-Mer, France.

[3]EIO UMR24, UPF/IRD/ILM/Ifremer, Labex CORAIL, Unité RMPF, Centre Océanologique du Pacifique, Vairao – BP 49 Vairao, Tahiti, Polynésie française.

Correspondence and requests for materials should be addressed to M.L. (email: mathieu.lutier@gmail.com) or to F.P. (email: fpernet@ifremer.fr)

Supplementary Note 1.

Temperature, salinity and O_2 saturation levels were stable across the experimental period and similar among pH conditions (Supplementary Table 1). Seawater was undersaturated with respect to calcite and aragonite when pH was below 7.3 and 7.6, respectively (Supplementary Table 1). However, parameters of carbonate chemistry were sometimes similar for different pH conditions. This reflects the difference in the frequency of measurements between the parameters (twice daily for pH and weekly for TA). Also, TA decreased slightly but linearly with increasing pH ($R^2 = 0.82$, slope = -0.08, $P < 0.001$) suggesting that seawater renewal was likely not sufficient to counteract both the uptake and the release of carbonate ions from net calcification at high pH and net dissolution at low pH, respectively (Supplementary Figure 2).

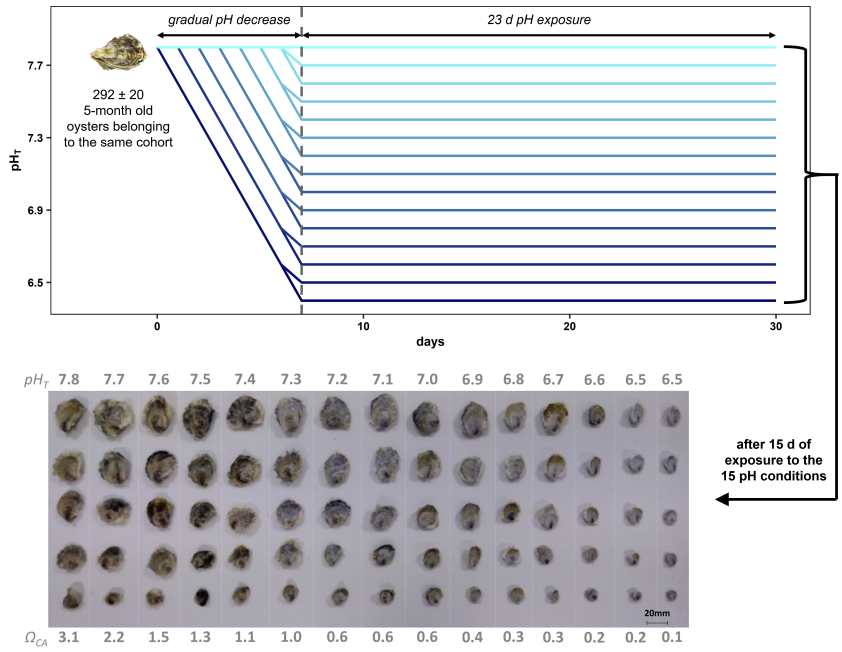

Supplementary Figure 1. Experimental design for the determination of oyster's reaction norms to pH. Each batch of oysters was exposed 23 d to one nominal pH condition after 7 d of gradual pH decrease at a rate of 0.2 unit d^{-1}. There were 15 nominal pH conditions. The aspect of 5 oysters is shown for each pH conditions at the end of the exposure period (23th day) in the lower panel.

1065

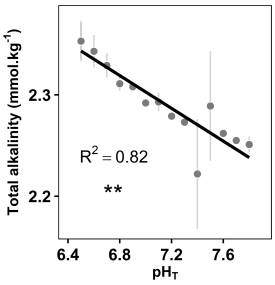

Supplementary Figure 2. Total alkalinity as a function of pH (total scale). Data are means ± SD values recorded during the 23 d of exposure. The significance level of the slope is presented using stars (P <0.001 ***, <0.01 **, <0.05 *, <0.1 ·).

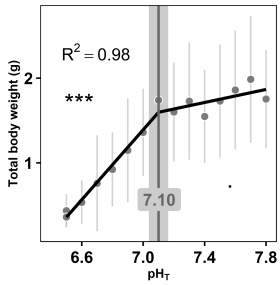

Supplementary Figure 3. Total body weight of oysters as a function of pH (pH on the total scale). Data are means ± SD. Tipping-point and its confidence intervals is shown in grey. The significance levels of the slopes are presented using stars (P < 0.001 ***, < 0.01 **, < 0.05 *, < 0.1 ·).

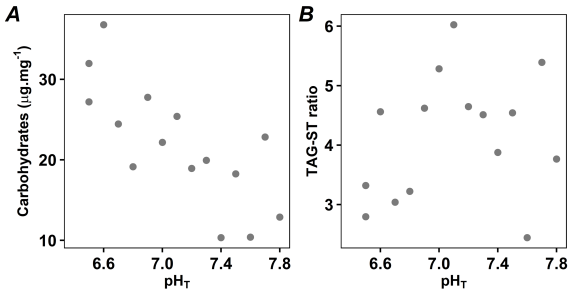

Supplementary Figure 4. Energy reserves of oysters as a function of pH (total scale). (A) total carbohydrates and (B) triacylglycerol/sterol ratio (TAG-ST). Relationships were not significant ($P > 0.05$).

Supplementary Table 1 Seawater parameters during the incubations. pH on the total scale (pH_T), calcite saturation state (Ω_{CA}), total alkalinity (TA), oxygen saturation (O_2), salinity (S) and temperature (T). *Average* represents the mean values between the onset and the end of the incubations. *Δ* represents the difference between the end and the onset of the incubations. Values are mean ± SD.

Nominal pH_T	**Average pH_T**	**Δ pH_T**	**Average Ω_{CA}**	**Δ Ω_{CA}**	**Δ TA** (µmol.kg^{-1})	**Δ O_2** (%sat)	**Δ NH_4^+** (µmol.L^{-1})	**Average S**	**Average T** (°C)
Blank	8.0±0.0	0.0	4.4±0.0	0.0	-3	2	0.0	35.7±0.0	21.7±0.1
Blank	8.0±0.0	0.0	4.3±0.0	0.0	1	1.7	-0.1	35.7±0.0	21.6±0.1
Blank	8.0±0.0	0.1	4.4±0.0	0.0	0	1.9	0.3	35.7±0.0	21.7±0.1
7.8	7.9±0.1	0.0	3.1±0.5	0.7	80	3	-1.1	35.7±0.0	21.7±0.1
7.7	7.6±0.1	0.1	1.7±0.3	0.4	65	6.5	-1.2	35.7±0.0	21.6±0.1
7.6	7.5±0.1	0.0	1.4±0.2	0.3	60	5	-1.0	35.7±0.0	21.7±0.1
7.5	7.4±0.1	-0.1	1.1±0.2	0.3	72	7.9	1.4	35.7±0.0	21.7±0.1
7.4	7.3±0.1	0.1	0.9±0.2	0.2	72	7.3		35.7±0.0	21.5±0.1
7.3	7.3±0.0	-0.2	1.0±0.0	0.0	61	6.1	-1.0	35.7±0.0	21.7±0.1
7.2	7.1±0.0	0.0	0.6±0.0	0.0	38	6.7	-0.8	35.7±0.0	21.7±0.1
7.1	7.1±0.0	0.0	0.6±0.0	0.0	44	5.5	-1.1	35.7±0.0	21.6±0.1
7.0	7.0±0.0	0.0	0.5±0.0	0.0	36	6.1	-2.0	35.7±0.0	21.7±0.1
6.9	6.9±0.0	0.1	0.4±0.0	0.0	19	5.5	-0.9	35.7±0.0	21.7±0.1
6.8	6.9±0.1	-0.1	0.4±0.1	-0.1	2	4.9	-1.0	35.7±0.0	21.6±0.1
6.7	6.8±0.1	-0.1	0.3±0.0	-0.1	13	3.1	-1.1	35.7±0.0	21.7±0.1
6.6	6.8±0.1	-0.2	0.3±0.1	-0.2	0	2.7	-0.6	35.7±0.0	21.6±0.1
6.5	6.7±0.1	0.1	0.3±0.1	-0.1	-12	2.4	-0.6	35.7±0.0	21.7±0.1
6.4	6.6±0.1	0.0	0.2±0.0	0.0	-18	1.5	-0.6	35.7±0.0	21.6±0.1

Supplementary Table 2 Seawater parameters measured during the experiment in each experimental tank, including three blanks without oysters. pH on the total scale (pH_T), total alkalinity (TA), oxygen saturation (O_2), salinity (S), temperature (T), calcite saturation state (Ω_{CA}), aragonite saturation state (Ω_{AR}), CO_2 partial pressure (pCO_2) and dissolved inorganic carbon (DIC) concentrations are shown (mean ± SD). pH, O_2, S and T were measured twice daily and TA was measured once a week.

Nominal	*Measured*					*Calculated*			
pH_T	**pH_T**	**TA** ($\mu mol.kg^{-1}$)	**O_2** (%sat)	**S**	**T** (°C)	**Ω_{CA}**	**Ω_{AR}**	**pCO_2** (μatm)	**DIC** ($\mu mol.kg^{-1}$)
Blank	8.0±0.1	2331±7	101.6±0.5	35.7±0.1	21.8±0.1	3.9±0.4	2.5±0.3	552±82	2111±31
Blank	8.0±0.1	2328±3	101.5±0.4	35.7±0.1	21.7±0.1	3.9±0.4	2.5±0.3	551±82	2108±29
Blank	7.9±0.2	2331±6	101.4±0.4	35.7±0.1	21.7±0.1	3.9±0.4	2.5±0.3	552±82	2111±29
7.8	7.8±0.1	2251±8	97.6±1.8	35.7±0.1	21.8±0.1	3.1±0.3	2.0±0.2	695±103	2082±33
7.7	7.7±0.1	2255±2	97.6±1.6	35.7±0.1	21.8±0.1	2.2±0.3	1.4±0.2	1070±161	2152±19
7.6	7.6±0.1	2262±2	96.7±2.6	35.7±0.1	21.7±0.1	1.5±0.0	1.0±0.0	1617±1	2217±2
7.5	7.5±0.1	2289±54	96.5±2.2	35.7±0.1	21.7±0.1	1.3±0.0	0.8±0.0	2091±49	2276±55
7.4	7.4±0.1	2222±54	97.1±2.1	35.7±0.1	21.7±0.1	1.1±0.1	0.7±0.1	2215±352	2219±66
7.3	7.3±0.0	2273±3	96.7±2.3	35.7±0.1	21.7±0.1	1.0±0.0	0.7±0.0	2644±4	2292±3
7.2	7.2±0.1	2279±3	96.8±2.2	35.7±0.1	21.8±0.1	0.6±0.0	0.4±0.0	4276±7	2371±3
7.1	7.1±0.1	2293±9	96.8±1.7	35.7±0.1	21.7±0.1	0.6±0.1	0.4±0.0	5067±671	2414±30
7.0	7.0±0.0	2292±3	97.2±1.5	35.7±0.1	21.7±0.1	0.6±0.1	0.4±0.0	5062±664	2413±27
6.9	6.9±0.1	2308±2	97.7±1.6	35.7±0.1	21.7±0.1	0.4±0.0	0.2±0.0	8160±1063	2536±38
6.8	6.8±0.1	2311±7	97.6±1.9	35.7±0.1	21.7±0.2	0.3±0.0	0.2±0.0	8777±26	2560±8
6.7	6.7±0.1	2329±12	98.2±1.3	35.7±0.1	21.7±0.1	0.3±0.0	0.2±0.0	11172±60	2656±13
6.6	6.6±0.1	2343±16	98.9±1.0	35.7±0.1	21.7±0.2	0.2±0.1	0.1±0.0	15691±3912	2813±135
6.5	6.5±0.2	2353±20	99.2±0.8	35.7±0.1	21.7±0.2	0.2±0.0	0.1±0.0	19865±4915	2953±164
6.4	6.5±0.3	2353±18	99.2±0.9	35.7±0.1	21.7±0.2	0.1±0.0	0.1±0.0	23079±5471	3054±183

Supplementary Table 3 Relative contribution of fatty acids to membrane. Their contribution (%) and Pearson's correlation to the first principal component (PC1) of the PCA are showed.

Average pH_T		Fatty acid (% total fatty acids)									
		14:0	**16:0**	**16:1n-7**	**18:0 dma**	**18:0**	**18:1n-9**	**18:1n-7**	**18:2n-6**	**18:3n-3**	**18:4n-3**
7.8		2.7	14.1	1.7	9.7	5.6	1.8	5.3	2.2	1.3	1.7
7.7		2.7	12.5	2.1	9.2	3.6	1.9	6.0	2.3	1.4	1.8
7.6		2.5	13.7	1.6	9.8	4.0	1.9	5.4	2.4	1.3	1.6
7.5		2.0	12.5	1.6	10.8	4.4	1.6	5.6	1.8	1.2	1.4
7.4		2.2	13.0	1.7	10.8	4.7	1.6	5.5	1.9	1.3	1.5
7.3		2.2	13.7	1.6	9.4	4.3	1.8	5.1	2.2	1.3	1.6
7.2		2.5	12.8	1.8	9.9	3.9	1.7	5.5	2.2	1.4	1.9
7.1		2.3	12.0	1.8	11.2	4.6	1.7	5.2	1.9	1.4	1.7
7.0		2.4	12.7	1.8	10.7	4.3	1.6	4.4	1.9	1.2	1.6
6.9		2.0	11.6	1.7	11.3	4.8	1.8	6.0	2.0	1.3	1.6
6.8		2.0	12.0	1.7	9.8	4.7	1.8	5.9	2.0	1.1	1.4
6.7		1.5	11.9	1.7	10.6	6.3	1.7	6.2	1.6	0.8	1.0
6.6		2.0	11.8	1.9	9.3	4.6	2.0	6.7	2.1	1.0	1.4
6.5		1.8	10.8	2.3	10.0	2.4	1.7	6.7	1.4	0.7	1.0
6.5		1.5	11.3	2.0	9.0	5.7	1.7	6.5	1.3	0.7	0.7
PCA	Contribution to PC1 (%)	1.9	13.6	0.5	0.7	0.0	0.0	4.6	1.7	1.1	1.8
	Correlation to PC1 (Pearson)	0.8	0.9	-0.8	0.2	0.0	0.0	-0.7	0.8	0.9	0.9

Average pH_T		Fatty acid (% total fatty acids)								
		20:1 dma	**20:0**	**20:1n-11**	**20:1n-7**	**20:4n-6**	**20:5n-3**	**22:2 $NMI_{i,j}$**	**22:5n-6**	**22:6n-3**
7.8		1.9	1.1	1.7	3.8	4.5	8.7	5.0	3.2	15.8
7.7		1.9	1.1	1.9	3.7	4.9	9.9	5.0	3.0	15.2
7.6		1.9	1.2	1.7	4.1	4.4	9.5	4.5	3.0	16.3
7.5		2.1	1.1	2.0	4.0	4.5	9.6	5.4	3.1	16.1
7.4		2.1	1.1	2.0	4.1	4.4	9.2	5.4	3.2	16.6
7.3		1.8	1.2	1.8	3.9	4.7	10.1	4.7	2.9	16.0
7.2		1.9	1.1	2.0	4.1	4.5	9.6	5.1	3.0	16.3
7.1		2.1	1.2	2.2	4.2	4.6	9.6	6.0	2.8	14.0
7.0		2.1	1.1	2.1	4.3	4.9	9.9	5.7	3.0	15.7
6.9		1.9	1.1	2.1	4.0	4.8	9.7	5.4	3.1	15.5
6.8		2.0	1.2	2.0	4.4	5.1	9.9	5.7	3.0	14.7
6.7		2.3	1.2	2.1	4.5	5.6	10.3	5.9	2.5	13.7
6.6		1.9	1.4	1.9	4.3	5.4	9.7	5.9	2.7	14.3
6.5		2.8	1.2	2.2	4.9	6.5	11.1	6.6	2.0	12.5
6.5		2.5	1.4	2.1	5.4	6.9	11.1	6.4	2.0	11.8
PCA	Contribution to PC1 (%)	1.2	0.1	0.2	3.2	11.8	6.1	5.8	2.8	43.0
	Correlation to PC1 (Pearson)	-0.8	-0.7	-0.6	-0.9	-1.0	-0.9	-0.9	0.9	1.0

Supplementary Table 4 Number of genes modelled against pH. Each step of filtering and the corresponding number of selected genes are specified.

WGCNA cluster of gene		correlated with pH	modelled & slope ≠ 0	model	
1	3380	1691	664	piecewise	567
				linear	97
2	723	343	148	piecewise	130
				linear	18
3	2073	623	242	piecewise	221
				linear	21